Ultrasound Assisted Synthesis of Mesoporous Materials Type MCM-41 in $scCO_2$

Hanu, A., Franke, K., Kareth, S. *, Petermann, M., Institute of Thermo and Fluid Dynamics, Faculty Machanical Engineering, IB 6/126, Ruhr-Universitaet Bochum, Universitaetsstr. 150, 44801 Bochum, Germany and
Puls, A., Rubotherm GmbH, 44799 Bochum, Germany
kareth@vtp.rub.de, Fax: +49-2343214277

INTRODUCTION

Siliceous crystalline molecular sieve MCM-41, member of M41S family of mesoporous materials, discovered almost two decades ago by the researchers from Mobil Oil Corporation, still attract the interest of scientists [1, 2]. MCM-41 possess a one-dimensional cylindrically pore system. It's a hexagonally (space group p6mm) ordered porous material with special features such as high surface area (up to 1000 m^2/g), pore diameter between 2 and 10 nm [2], and pore volume up to 1.3 ml/g. Thanks to its characteristics, MCM-41 have been proved to be a suitable matrix, after activation with different active species, for applications in different fields like catalysis [3-5] and photocatalysis [6, 7], environmental depollution [8-11], controlled drug release [12], sensors and biosensors [13].

The proposed mechanism for the synthesis of MCM-41 materials is a self-assembled liquid crystal mechanism (LCT), involving sol-gel precursors which determinate the formation of hexagonally packed micelle structure [2]. Four main components are necessary for the synthesis: a silica source, a template agent, a catalyst and solvent. Usually, ordered MCM-41 structure, using silicon alkoxides (e.g. TEOS – tetraethylorthosilicate) and quaternary ammonium salts (e.g. CTAB – cetyltrimethylammonium bromide) as structure agent, is obtained at pH < 2 [14] and > 10 [1, 2]. In the alkaline route, which leads to more stable and ordered materials because of a good condensation of silica, surfactant (S) and silicates (I), are organized by strong S^+I^- interaction. In the acidic route, well known for generating a wide variety of morphologies of products [15, 16], the silica species are positively charged as $\equiv SiOH_2^+$ and the interaction with the surfactant is intermediated by the counter ion ($S^+X^-I^+$). In the pH range 3-7 disordered mesostructures are obtained because of the formation of an excess amount of surfactant accompanied by the counter ion (S^+X^-) [17].

The conventional hydrothermal synthesis of MCM-41 is taking place under autogenic pressure during a relative long time (several days). Unconventional methods, like microwave-assisted synthesis, capture the attention of researchers in the last years because of its advantage such as fast synthesis time and low energy consumption [18]. Less attention was paid to the ultrasound assisted synthesis of this type of material. Only few studies were dealing with ultrasound supported synthesis [19, 20]. Recent studies revealed that, thanks to the cavitations effect caused by ultrasounds, the local temperature and pressure are raising, conferring to the sonicated solution new properties, which may determinate a enhancement of hydrolysis and condensation of silica species, leading to obtain ordered MCM-41 in less than 5 min [21].

Typically, the assistance of supercritical CO_2 ($scCO_2$) – low cost, non-toxic, non-flammable solvent, having accessible critical temperature and pressure, low surface tension and dynamic viscosity – was used with the aim to deposit different active groups on the pore surface of MCM-41 [22], to incorporate metals in the channels walls [23], or to remove the surfactant from the pores [24].

No information regarding the synthesis of MCM-41, using CTAB as template agent, in $scCO_2$ and ultrasound $scCO_2$ are available in the literature. Only few studies are dealing with the synthesis of this material in sub– and supercritical CO_2, but in the presence of a nonionic triblock copolymer (polyethylene oxide-polypropylene oxide-polyethylene oxide, $EO_{106}PO_{70}EO_{106}$) as direct structure agent [25]. Chun et al. highlighted that under $scCO_2$ conditions disordered mesoporous structures are formed [25].

Our studies were focused on the synthesis of type MCM-41 materials in supercritical CO_2 and on the ultrasound assisted synthesis in $scCO_2$. The influence of pressure and ultrasound intensity on the structural features was studied. All studies were carried out using the same temperature and reaction time. Detailed characterization of the samples was performed by XRD, N_2 adsorption/desorption measurements, FTIR and SEM.

Unexpected ordered type MCM-41 mesoporous materials were obtained despite of the low pH value of the reaction medium (pH ≈ 3), close to the isoelectric point of silica. The ordering degree is increasing with increasing $scCO_2$ pressure. Furthermore, the presence of ultrasound in the reaction medium causes a further enhancement of pore ordering.

MATERIALS AND METHODS

Reagents

For the synthesis of mesoporous materials type MCM-41 the following reagents were used: cetyltrimethylammonium bromide (CTAB) – Merck; tetraethylorthosilicate (TEOS) – Merck; ethyl alcohol (EtOH) – J.T. Baker; ammonia 25 % solution (NH_3) – Riedel–de Haën.

The experiments in $scCO_2$ were carried out using CO_2, 99.9 % purity, purchased from Yara.

Synthesis of MCM-41 mesoporous material at room conditions and under $scCO_2$

Mesoporous silicate MCM-41, (designated as S), reference sample, was prepared according to the procedure presented by Grün et al. [26] and Liu et al. [27], respectively. Briefly, cetyltrimethylammonium bromide was dissolved in a mixed solution of water, ethanol and ammonia for 10 min under stirring. Then tetraethylorthosilicate was added, resulting in a gel with molar composition: $1TEOS : 0.3CTAB : 11NH_3 : 54EtOH : 115H_2O$. After 1 h reaction at 40 °C, the sample was filtrated, washed, dried at room temperature and calcined at 550 °C for 24 h.

The samples synthesized under supercritical CO_2, showed the same molar composition. In order to study the influence of $scCO_2$ on the properties of MCM-41, glass sample holders covered with perforated lids containing mixed solutions of template agent, H_2O, NH_3, EtOH and TEOS were quickly introduced in a specially design high pressure view cell (Fig. 1). The cell with a maximum inner volume of approx. 330 ml was designed to operate up to 750 bar and 200 °C. The temperature inside the view cell was adjusted with the help of an electrical heater equipped with cartridge heaters.

The cartridge heaters were placed directly in the view cell body. Two thermocouples (NiCr-Ni type K) were used to measure the temperature inside the view cell and on the surface of the cartridge heaters. A transducer Dynisco MDA 420-1/2-1M was measuring the pressure inside the cell. Pressure was raised by introducing compressed CO_2 to the desired value.

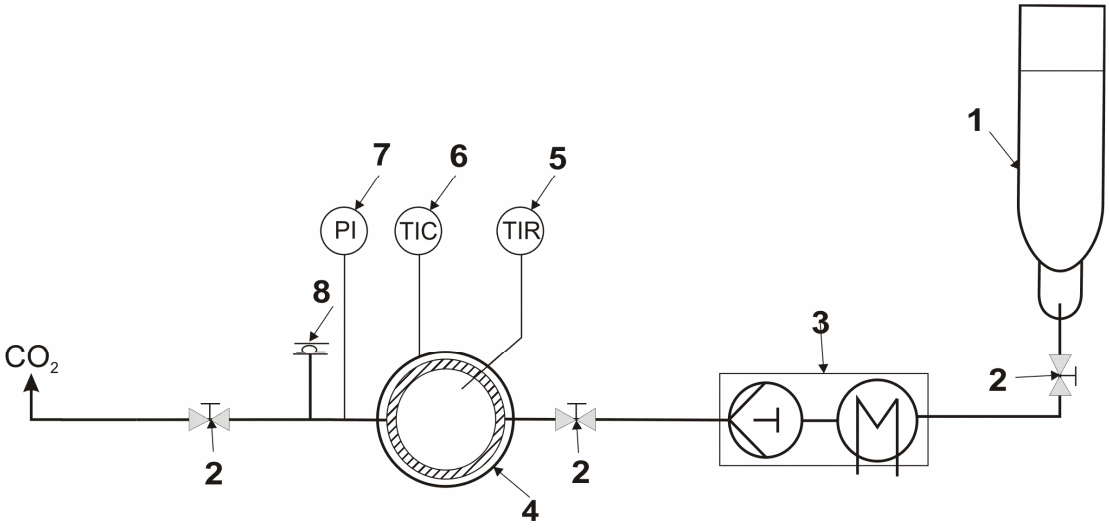

Fig. 1: Schematic of high pressure plant: 1 – CO_2 supply; 2 – needle valve; 3 – compressor; 4 – view cell including ultrasound sonotrode; 5 – temperature indicator regulator (TIR); 6 – temperature indicator controller (TIC); 7 – pressure indicator (PI); 8 – bursting disc.

The experiments were carried out at 40 °C, and different pressures (64 – 200 bar) in sub- and supercritical CO_2 medium. After 1 h the pressure was slowly decreased to atmospheric pressure. The resulting solid material was filtrated, washed with distilled water, dried at room temperature and calcined at 550 °C for 24 h.

In the ultrasound assisted synthesis in $scCO_2$, the samples were obtained in the same way as described above, additionally a sonotrode (Weber Ultrasonics, 40 kHz, max. 150 W) mounted axially inside the view cell, was used.

Characterization

The obtained samples were characterized using X-ray diffraction (XRD), N_2 adsorption/desorption isotherms, scanning electron microscopy (SEM), Fourier transform infrared - attenuated total reflectance spectroscopy (FTIR - ATR).

The X-ray patterns were recorded on a PANalytical powder diffractometer (40 kV, 30 mA) using Ni filtered Cu_α (0.154 nm) radiation.

N_2 adsorption/desorption measurements were performed on a BELSorp-Mini II instrument, automated gas adsorption system, using N_2 as absorbate at -196 °C. Prior to the measurements the samples were degassed. The evaluation was made using the BElmaster software Vers. 6.0. Pore diameter was obtained using the Barrett-Joyner-Halenda (BJH) method and specific surface area was determined with the Brunauer-Emmett-Teller (BET) method, in the range of relative pressure 0.05 – 0.35. The total pore volume was taken at a value of 0.99 relative pressure.

The SEM images were obtained, after the samples were sputtered with a thin film of gold, using a LEO (Zeiss) 1530 Gemini FESEM microscope operating at an voltage of 0.2 – 30 kV. FTIR – ATR spectra were performed with a Bruker Tensor 27 spectrometer. The samples were analyzed without preliminary preparation. In order to obtain a good contact between the solid sample and ZnSe crystal, the pressing device was used. For every sample, 25 scans were taken automatically.

RESULTS

The XRD patterns (not shown) of the reference samples (noncalcined – S_{non} and calcined S) synthesized under ambient pressure proved the hexagonal arrangement of the obtained materials. Strong diffraction peaks attribute to (100) reflection are present at 2θ = 2.40 for S_{non} and 2θ = 2.48 for S. Another peak indexed to (110) interplanar spacing is present for both samples, evidence of good pore ordering.

For samples synthesized under $scCO_2$ it's obvious that the ordering of the material is decreasing (Fig. 2A). The sample obtained at 64 bar (designated S_{64}) presents no peak in the diffractogram, because of the very low pore ordering. Beginning with 84 bar (sample designated S_{84}) a shoulder is appearing in the interval of 2θ = 1.5 – 3 in the diffractograms. With increasing pressure the apparition of a broad peak (100) around 2θ = 2.44 can be observed – sample obtained at 120 bar (designated S_{120}).

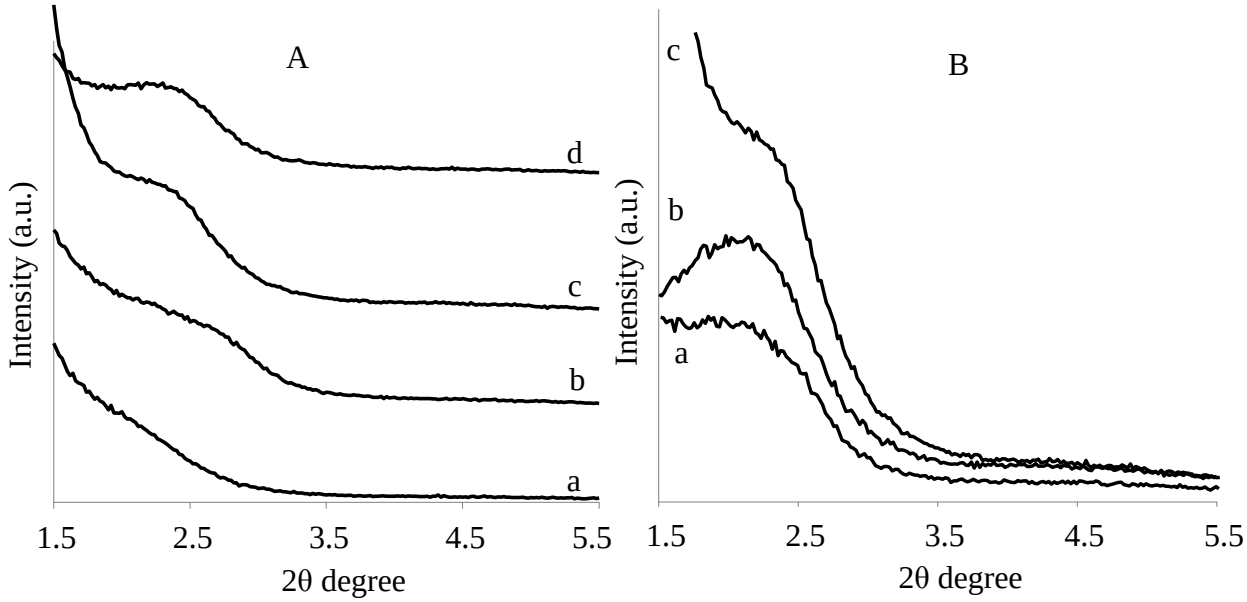

Fig. 2: XRD patterns of obtained noncalcined samples: A - synthesis under CO_2: a – 64 bar; b – 84 bar; c – 120 bar; d – 200 bar and B - compared samples under CO_2 and assisted ultrasound CO_2: a – 120 bar, 15 W; b – 120 bar, 20 W; c – 120 bar.

In the pattern for the sample synthesized at 200 bar (designated S_{200}) the peak attributed to (100) reflection becomes narrow, proof of an increase in the ordering degree of the material.

The use of ultrasounds during the synthesis under CO_2 atmosphere, leads to a strong increase of the structural ordering. In the patterns of the samples obtained at 120 bar with ultrasounds power 15 W and 25 W (designated S_{12015}, S_{12025}, respectively) a narrow peak corresponding to (100) reflection can be observed, as well as the peak attributed to (110) reflection that can be detected for sample S_{12025} (Fig. 2B). Increasing of ultrasound power leads to a shift of the major peak at lower values of 2θ = 2.16 for S_{12015} and 2θ = 2.08 for $S_{12025,}$ respectively, which denoted an increasing of lattice constant – a_0 (see Table I).

Excepting S_{12015}, N_2 adsorption/desorption isotherms (Fig. 3) of the obtained samples, under $scCO_2$, $scCO_2$ and ultrasounds, respectively, are type IV in the IUPAC classification, typical for mesoporous materials [28].

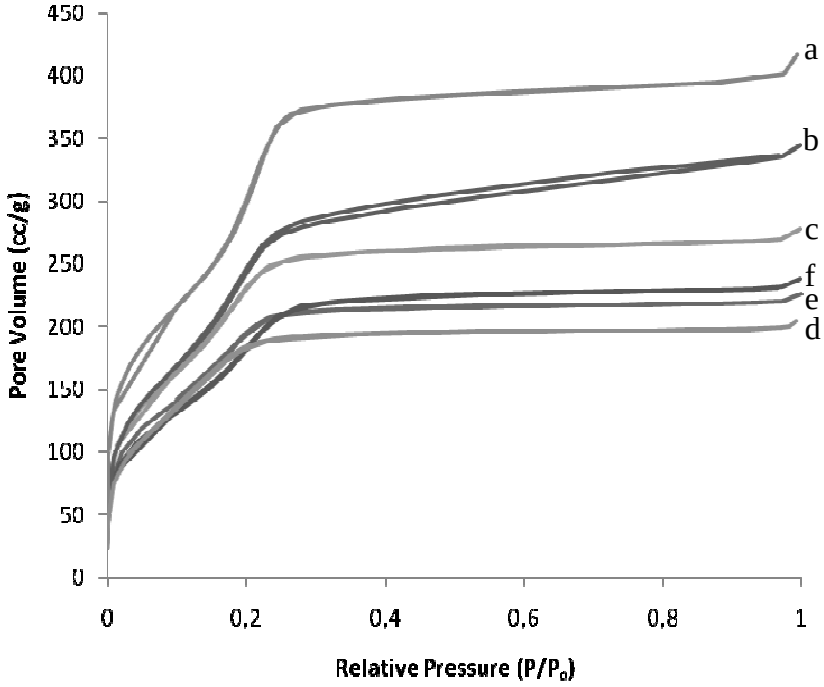

Fig 3: N_2 adsorption/desorption isotherms of the samples synthesized at: a – room conditions; b – 120 bar; c – 200 bar; d – 120 bar and 15W; e – 120 bar and 20W; f – 120 bar and 25W.

The capillary condensation steps are present at a relative pressure (P/P_0) between 0.1 and 0.3. This step start at a relative pressure lower then 0.2 for samples S_{120}, S_{200}, S_{12020}, suggesting a broad pore size distribution. For sample S_{12025} the capillary condensation step starts at P/P_0 = 0.2, indicating a narrow distribution of the pore size (as well as in the reference sample – S). The type H4 hysteresis loop, associated with slit-like pores [28] is present for sample S_{120}. All other samples are not presenting hysteresis loop due to small mesopores smaller than 4 nm. The features of some of the obtained samples are presented in Table 1.

Table 1: Characteristics of the porous materials obtained under $scCO_2$ an ultrasound assisted $scCO_2$.

Sample name	S_{BET} (m^2/g)	Total pore volume (cc/g)	Pore diameter (nm)	Particle size (μm)	a_0* (nm)	δ** (nm)
S	930	0.640	2.75	0.5	4.24	1.49
S64	-	-	-	0.6 agglomeration	-	-
S_{84}	-	-	-	agglomeration	3.80	-
S_{120}	775	0.529	2.73	agglomeration	4.24	1.51
S_{200}	705	0.425	2.41	agglomeration	4.31	1.90
S_{12015}	653	0.314	1.92	agglomeration	4.54	2.62
S_{12020}	644	0.346	2.14	agglomeration	-	-
S_{12025}	589	0.364	2.47	agglomeration	4.71	2.24

* - calculated from the equation: $a_0 = 2d_{100}/\sqrt{3}$ [29]
** - wall thickness calculated from the equation: $\delta = a_0 - D(BJH)$ [30]

Synthesis in the presence of liquid CO_2 and $scCO_2$ leads to formation of porous materials with lower specific surface area than the reference material. From the adsorption/desorption data (Table 1.) a decrease in the surface area with increasing pressure can be seen. Also, the total pore volume and the pore diameter are in decline, suggesting a degradation of the porous characteristics of the obtained materials. The degradation of the porous characteristics can be explained by the pH of reaction medium.

In $scCO_2$ the pH of the aqueous solution is decreasing until pH ≈ 3. At this pH value, near the isoelectric point of silica, the structure of MCM-41, synthesized in normal conditions, or autoclave, with CTAB is highly disordered, exhibiting no peak in the XRD diffractograms. Silica species are negative charged in neutral and basic solution, and the mechanism of formation of mesoporous silica is attributed to the electrostatic interaction S^+I^- between positively charged surfactant ($S^+ = CTA^+$) and negatively charged silica (I^-). Previous research asset that in the vicinity of the isoelectric point of silica the framework mesopores disappear and a disorder texture is formed because the electrostatic interaction are not performed for the assembly [32]. In the range of pH between 3 and 7 the interaction between silica and surfactant micelles are disturbed by the formation of an excess amount of surfactant accompanied with the counter ion, in our case CTA^+Br^- [31]. The presence of the ultrasounds in the synthesis medium leads to a further decrease in the specific surface area, pore volume and pore diameter. S_{BET} is decreasing, but total pore volume and pore diameters (implicitly the wall thickness) are increasing with increasing the ultrasound power.

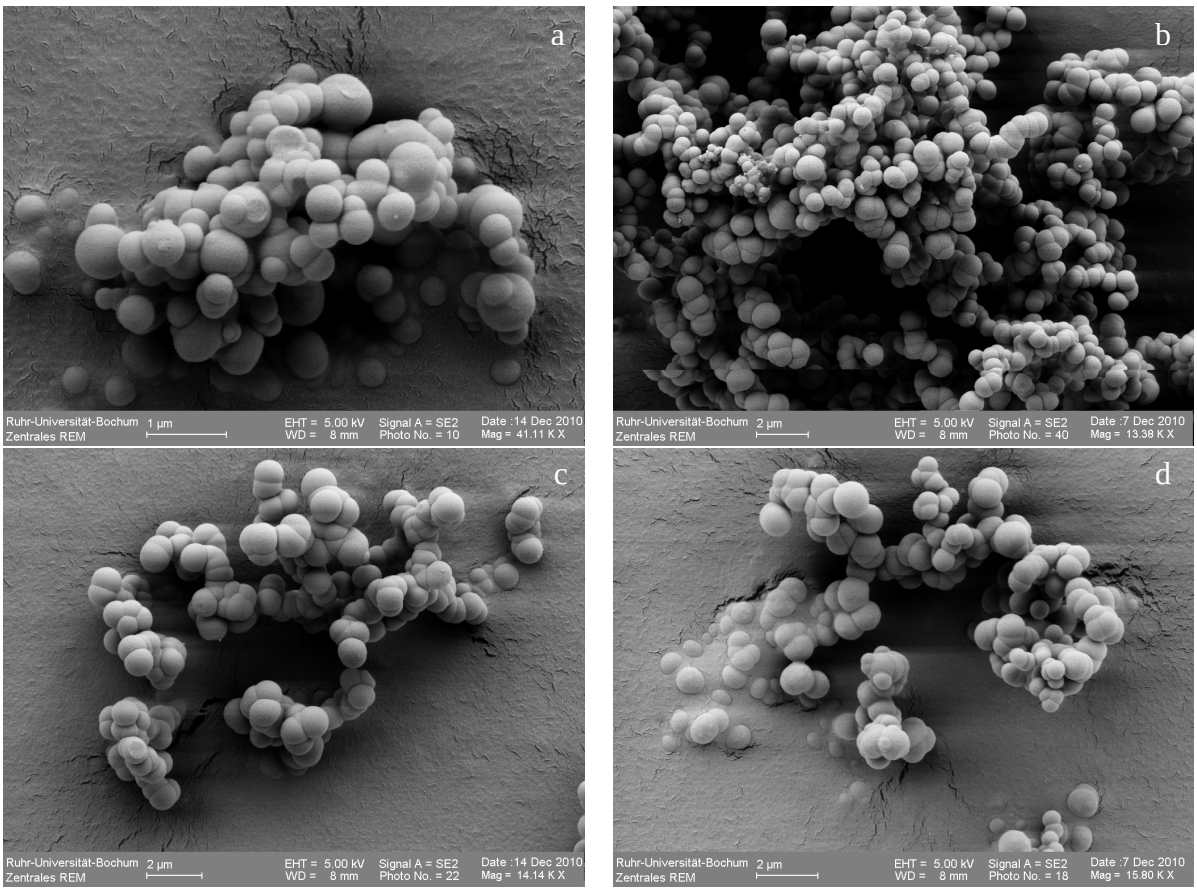

Fig. 4: SEM images of samples: a – S; b – S_{84}; c – S_{120}; d – S_{200}.

SEM pictures of reference material S show spherical morphology of the particles (Fig. 4 – a) with particle size around 0.5 µm. Applying high pressure the particles tend to fusion, forming agglomeration (Fig. 4 – b, c, d). No important differences between the particle morphology are obtained at different pressure, suggesting that only the pressure influence the particles morphology, and not the pressure value. The same observations were made in the case of the samples obtained under ultrasounds and CO_2 atmosphere. Fusion of the particle is caused by both, pressure and ultrasound presence.

CONCLUSIONS

The synthesis of ordered type MCM-41 materials using TEOS as silica source and CTAB as structure template agent is possible at a pH near the isoelectric point of Si, due to the presence of supercritical CO_2. Experimental results indicate that the structure ordering degree is strongly dependent of the pressure value, increasing with the pressure rise. Ultrasound presence in the synthesis medium leads to a further improvement of the structural ordering, due to the enhancement of silicon hydrolysis rate. The pore ordering is closely correlated with the ultrasound intensity. Despite of low pH (≈ 3) of $scCO_2$, which favors the formation of disordered structure, it was possible to obtain ordered MCM-41 material using high pressure (200 bar), ultrasound and short synthesis time (1 h).

REFERENCES

[1] KRESGE, C.T., LEONOWICZ, M.E., ROTH, W.J., VARTULI, J.C., BECK, J.S., Nature, Vol. 359, **1992,** p. 710

[2] BECK, J.S., VARTULI, J.C., ROTH, W.J., LEONOWICZ, M.E., KRESGE, C.T., SCHMITT, K.D., CHU, C.T.W., OLSON, D.H., SHEPPARD, E.E., McCULLEN, S.B., HIGGINS, J.B., SCHLENKER, J. L., J. Am. Chem. Soc., Vol. 114, **1992,** p. 10834

[3] LUAN, Z., XU, J., HE, H., KLINOWSKI, J., KEVAN, L., J. Phys. Chem. B, Vol. 100, **1996,** p. 19595

[4] CORMA, A., NAVARRO, M.T., PARIENTE, J. P., J. Chem. Soc. Chem. Comm., Vol. 147, **1994,** p. 17

[5] REDDY, K.M., MOUDRAKOVSKI, I., SAYARI, A., J. Chem. Soc., Chem. Comm., Vol. 9, **1994,** p. 1059

[6] ZHENG, S., GAO, L., ZHANG, Q., GUO, J., J. Mater. Chem., Vol. 10, **2000,** p. 723

[7] DAVYDOVA, L., REDDYA, E.P., FRANCEA, P., SMIRNIOTIS, P. G., Journal of Catalysis, Vol. 203, **2001**, p.157

[8] HU, X., QIAO, S., ZHAO, X.S., LU, G.Q., Ind. Eng. Chem. Res., Vol.40, **2001,** p. 862

[9] JUANG, L.C., WANG, C.C, LEE, C. K., Chemosphere, Vol. 64, **2006,** p. 1920

[10] KWONG, C.W., CHAO, Y.H., HUI, K.S.,WAN, M.P., Atmospheric Environment, Vol. 42, **2008**, p. 2300

[11] HANU, A.M., LIU, S., MEYNEN, V., COOL, P., POPOVICI, E., VANSANT, E. F., Microporous and Mesoporous Materials, Vol. 95, **2006**, p. 31

[12] VALLET-REGI, M., RÁMILA, A., PÉREZ-PARIENTE, R. P., DEL REAL, J., Chem. Mater., Vol. 13, **2001,** p. 308

[13] NEUMANN, R., KHENKIN, A. M., Chem Commun., Vol. 23, **1996**, p. 2643

[14] HUO, Q., MARGOLESES, S.I., CIESLA, U., FENG, P., GIER, D.E., SIEGER, P., LEON, B.F.R., PETROFF, P.M., SCHÜTH, F.,STUCKY, G. D., Nature, Vol. 368, **1994,** p. 317
[15] YANG, H., COOMBS, N.,OZIN, G. A., Nature, Vol. 386, **1997,** p. 692
[16] OZIN, G.A., YANG, H., SOKOLOV, I.,COOMBS, N., Adv. Mater., Vol. 9, **1997,** p. 662
[17] MUTO, S., IMAI, H., Microporous and Mesoporous Materials, Vol. 95, **2006,** p. 200
[18] CAO, Y., WEI, H., XIA, Z., Trans. Nonferrous Met. Soc. China, Vol. 19, **2009,** p. 656
[19] TANG, X., LIU, S., WANG, Y., HUANG, W., SOMINSKI, E., PALCHIK, O., KOLTYPIN, Y., GEDANKEN, A., Chem. Commun., Vol. 21, **2000**, p. 2119
[20] HANU, A.M., POPOVICI, E., COOL, P., VANSANT, E. F., Recent Progress in Mesostructured Materials, D. Zhao, S. Qiu, Y. Tang and C. Yu (Editors), **2007**, Elsevier B.V., p. 169
[21] VETRIVEL, S., CHEN, C.T.,KAO, H. M., New J. Chem., Vol. 34, **2010,** p. 2109
[22] CHATTERJEEA, M., IKUSHIMA, Y., Studies in Surface Science and Catalysis, Vol. 156, **2005,** p. 427
[23] LI, S., XU, Q., CHEN, J., GUO, Y., Ind. Eng. Chem. Res., Vol. 47, **2008,** p. 8211
[24] KAWI, S., Chem Commun., Vol. 13, **1998**, p. 1407
[25] CHUN, B.S., PENDLETON, P., BADALYAN, A., PARK, S.Y., Korean Journal of Chemical Engineering, Vol. 27, **2010,** p. 983
[26] GRÜN, M., UNGER, K.K., MATSUMOTO, A., TSUTSUMI, K., Microporous and Mesoporous Materials, Vol. 27, **1999,** p. 207
[27] LIU, S., COOL, P., COLLART, O., VAN DER VOORT, P., VANSANT, E. F., LEBEDEV, O. I., VAN TENDELOO, G., JIANG, M., J. Phys. Chem. B, Vol. 107, **2003,** p. 10405
[28] IUPAC, Recommendations, Pure Appl. Chem., Vol. 57, **1985,** p. 603
[29] CIESLA, U., SCHÜTH, F., Microporous and Mesoporous Materials, Vol. 27, **1999,** p. 131
[30] YU, J., SHI, J.L., WANG, L.Z., RUAN, M.L., YAN, D.S., J. of Materials Science Letters, vol. 20, **2001,** p. 289
[31] MUTO, S., IMAI, H., Microporous and Mesoporous Materials, Vol. 95, **2006,** p. 200